Specific heat capacity in the low-density regime of asymmetric nuclear matter

R. Aguirre*

Departamento de Fisica, Facultad de Ciencias Exactas, Universidad Nacional de La Plata, and IFLP, CCT La Plata, CONICET, La Plata, Argentina

(Received 12 September 2011; published 20 January 2012)

Thermal and isospin composition effects on the heat capacity of infinite nuclear matter are studied within the binodal coexistence region of the nuclear phase diagram. Assuming the independent conservation of both proton and neutron densities, a second-order phase transition is expected, leading to a discontinuous behavior of the heat capacity. This discontinuity is analyzed for the full range of the thermodynamical variables consistent with the equilibrium coexistence of phases. Two different effective models of the nuclear interaction are examined in the mean-field approximation: the nonrelativistic Skyrme force and the covariant QHD formulation. We found qualitative agreement between both descriptions. The discontinuity in the specific heat per particle is finite and decreases with both the density of particles and the isospin asymmetry. As a byproduct, the latent heat for isospin-symmetric matter is considered.

DOI: 10.1103/PhysRevC.85.014318 PACS number(s): 21.65.Cd, 21.30.Fe, 21.65.Mn, 64.70.F−

I. INTRODUCTION

The in-medium nuclear interaction gives rise to a complex thermodynamical phase diagram. Several phases are expected to take place as temperature and density are varied, for instance superfluid, superconducting, boson condensed, Bose-Einstein condensed deuteron, and quark deconfined phases. Along these thermodynamical changes some constraints must be fulfilled, such as conservation of baryonic number, electric charge, etc., which have severe consequences on the evolution of the state of matter.

As a typical situation, we mention the liquid-gas phase transition (LGPT), expected to occur in the low-density, low-temperature regime of nuclear matter. It has been subject of study for a long time, and it has received renewed attention in recent years [1–5]. The theoretical treatment requires an interesting combination of quantum statistical approaches with models of the nuclear interaction. Comparison with empirical results can be done in the field of ion collision experiments—see for example Ref. [6]—as well as with observational data concerning the thermal equilibration of proto-neutron stars [7,9]. Different situations prevent a direct application of the theoretical predictions; for instance, finite size effects are significant in heavy-ion collisions. Furthermore, the very short characteristic times of the reactions makes the applicability of equilibrium thermodynamics dubious. On the other hand, the possible frustration of the binodal transition and the appearance of a nonhomogeneous phase near the surface layer of neutron stars complicate the interpretation of the transport properties of star matter.

It is clear that detailed calculations should take into account a multitude of specific effects. However, with the purpose of highlighting the basic features, some simplified calculations are admissible and they serve as a useful reference for more complex statements [5].

The existence of more than one conserved charge is a feature of the above-mentioned situations. A phase transition taking place under such requirements has distinctive consequences, such as the fact that the conserved charges do not distribute uniformly among the coexisting phases [10]. Certainly, the isospin fractionation observed in multifragmentation experiences [11] could be the fingerprint of a LGPT occurring after the collision.

A variety of models and approximations have been used to describe the nuclear equation of state. The combination of mean-field approaches with effective models, adjusted to reproduce the nuclear phenomenology, offers the advantages of simple calculations and reliable results. Among the most used representations of the nuclear force, we mention the nonrelativistic Skyrme model and the covariant formulation known as quantum hadrodynamics (QHD). They have dissimilar foundations—a density-dependent nucleon-nucleon potential and a covariant exchange of mesons are respectively used—but eventually both give rise to an energy density functional. Within this formulation, they can be fairly compared.

The fact that nuclear systems could have more than one conserved charge has noticeable consequences on the evolution of thermodynamical instabilities. Indeed, there is a change in the order of the transition, allowing a continuous variation of the thermodynamic potentials. Discontinuities are relegated to the first derivatives, corresponding, for instance, to the compressibility and heat capacity of the system.

It is worthwhile to mention that the inclusion of other effects, such as the Coulomb and surface-tension forces, could change dramatically this description [8].

In the present work we intend to study the behavior of the heat capacity of infinite nuclear matter within the coexistence region. The heat capacity is of great significance in, for instance, the evaluation of the rate of change of temperature through the outer shell of young neutron stars [9]. It has also been studied in relation to nuclear multifragmentation, where it is considered to be an indicator of the LGPT [12,13]. A statistical model of multinucleon clusters is frequently used

*aguirre@fisica.unlp.edu.ar

for this purpose, focusing the calculations on the low-isospin asymmetry regime. The upper limit for the temperature is determined by a characteristic value, of the order $T \sim 10$ MeV, for which clusters start to dissolve.

In this work we explore a wide range of temperature, particle-density, and isospin composition, which can be easily combined in a mean-field calculation. We examine two effective models of the nuclear interaction: the Skyrme potential and the QHD relativistic formulation.

This article is organized as follows. The general features of the models are presented in the next section, and the results are shown and discussed in Sec. III. A final summary is given in Sec. IV.

II. THE NUCLEAR LIQUID-GAS PHASE TRANSITION IN DIFFERENT MODELS

In order to check the generality of the results found, two phenomenological models of the nuclear force have been used. The first is the well known Skyrme model, where medium effects are included through density-dependent parameters for the nucleon-nucleon potential. As an alternative formulation, we choose the QHD model. Here the interaction is mediated by meson fields, which are evaluated in a self-consistent way.

In both cases the isospin composition can be easily handled. It can be parameterized by the asymmetry fraction $w = (n_2 - n_1)/n$, with n_1 and n_2 standing for the particle number density of protons and neutrons respectively, and $n = n_1 + n_2$ is the total nucleon density.

We assume both proton and neutron numbers are conserved independently. Hence, different chemical potentials μ_a can be assigned to each isospin component. The statistical distribution function can be written $f_a(T, p) = \{1 + \exp\beta[\varepsilon_a(p) - \mu_a]\}^{-1}$, where the particle energy spectrum $\varepsilon_a(p)$ is provided by the proposed model.

Throughout this article we use units such that $c = 1, \hbar = 1$, and $k_B = 1$.

A. The Skyrme model

The Skyrme model is a well known effective formulation of the nuclear interaction [14]. It consists of a basic Hamiltonian with contact potentials and density-dependent coefficients,

$$
\begin{aligned}
v_{\rm Sky}(r_1, r_2) = {} & t_0(1 + x_0\, P_\sigma)\delta(r_1 - r_2) + \frac{1}{2}t_1(1 + x_1\, P_\sigma)[\overleftarrow{q}^2\ \delta(r_1 - r_2) + \overrightarrow{q}^2\ \delta(r_1 - r_2)] \\
& + t_2(1 + x_2\, P_\sigma)\ \overleftarrow{q}\cdot\delta(r_1 - r_2)\ \overrightarrow{q} + \frac{1}{6}t_3(1 + x_3\, P_\sigma)\delta(r_1 - r_2)\rho^\gamma[(r_1 + r_2)/2] \\
& + i\,W_0(\sigma_1 + \sigma_2)\cdot\ \overleftarrow{q}\ \times\delta(r_1 - r_2)\ \overrightarrow{q},
\end{aligned}
$$

where σ_k represent the Pauli matrices for spin, $P_\sigma = (1 + \sigma_1 \cdot \sigma_2)/2$ is the spin exchange operator, and $q = -i(\nabla_1 - \nabla_2)/2$ is the relative momentum operator. Several parametrizations have been given, according to the applications planned. They cover cases from exotic nuclei to stellar matter.

By taking the Hartree-Fock expectation value from this force, an energy density functional is obtained, which for infinite homogeneous nuclear matter is given by

$$
\mathcal{E}_{\rm Skm} = \delta_s \sum_j \frac{K_j}{2m_j^*} + \frac{1}{16}(a_0 + a_2 w^2)\, n^2. \tag{1}
$$

The factor $\delta_s = 2$ takes account of the spin degeneracy, and the kinetic density of particles with isospin j ($j = 1,2$ for protons and neutrons, respectively) is given by

$$
K_j = \frac{1}{(2\pi)^3}\int d^3p\ p^2 f_j(T, p). \tag{2}
$$

Here, $f_j(T, p)$ is the Fermi occupation number for the isospin component j at temperature T. The effective nucleon mass m_j^* for this state is given by

$$
\frac{1}{m_j^*} = \frac{1}{m} + \frac{1}{4}\, n\,(b_0 - b_2 w I_j), \tag{3}
$$

where m represents the in-vacuum degenerate nucleon mass and $I_j = (-1)^{1+j}$.

The density-dependent coefficients a_0, a_2 and b_0, b_2 can be expressed in terms of the standard parameters of the Skyrme model:

$$
\begin{aligned}
& a_0 = 6t_0 + t_3 n^\gamma, \quad b_0 = [3t_1 + t_2(5 + 4x_2)]/2, \\
& a_2 = -2t_0(1 + 2x_0) - t_3(1 + 2x_3)n^\gamma/3, \quad b_2 = [t_2(1 + 2x_2) \\
& \qquad - t_1(1 + 2x_1)]/2.
\end{aligned}
$$

Within a Landau-Fermi liquid scheme, the particle spectra can be obtained by the functional derivatives $\varepsilon_{\rm as}(p) = \delta\mathcal{E}_{\rm Skm}/\delta f_{\rm as}(T, p)$. In such a way, the following result is obtained [15]:

$$
\begin{aligned}
\varepsilon_j(p) &= \frac{p^2}{2m_j^*} + \frac{1}{8}v_j + \Delta\varepsilon, \\
v_j &= (a_0 - a_2 w I_j)\, n + \delta_s \sum_k (b_0 + I_j I_k b_2) K_k, \\
\Delta\varepsilon &= [3n^2 - (1 + 2x_3)n^2 w^2]\sigma t_3 n^{\sigma-1}/48.
\end{aligned}
$$

The set of self-consistent equations is completed with the relation between the conserved particle numbers and the

corresponding chemical potentials:

$$n_j = \frac{\delta_s}{(2\pi)^3}\int d^3p\ f_j(T,\,p). \tag{4}$$

B. QHD model

This is a model of the covariant field theory, proposed to deal with in-medium nuclear properties [16]. The interaction is mediated by isoscalar mesons σ and ω_μ; the first one can be considered as a resonant state. In the present case the isovector mesons ϕ and ρ_μ are also included, as well as polynomial terms in the σ field.

The lagrangian density is

$$\begin{aligned}\mathcal{L} = {}& \bar{\Psi}\,(i\ \partial\!\!\!/ - M + g_s\,\sigma + g_c\,\tau\cdot\phi - g_w\ \omega\!\!\!/ - g_r\tau\cdot\ \rho\!\!\!/)\,\Psi \\ & + \frac{1}{2}\left(\partial^\mu\sigma\,\partial_\mu\sigma - m_s^2\sigma^2\right) - \frac{A}{3}\,\sigma^3 - \frac{B}{4}\,\sigma^4 \\ & + \frac{1}{2}\left(\partial^\mu\phi\cdot\partial_\mu\phi - m_c^2\phi^2\right) - \frac{1}{4}F^{\mu\nu}F_{\mu\nu} \\ & + \frac{1}{2}m_w^2\omega^2 - \frac{1}{4}R^{\mu\nu}\cdot R_{\mu\nu} + \frac{1}{2}m_r^2\rho^2,\end{aligned}$$

where $\Psi(x)$ is the isospin multiplet nucleon field, $F_{\mu\nu} = \partial_\mu\omega_\nu - \partial_\nu\omega_\mu$, $R_{\mu\nu} = \partial_\mu\rho_\nu - \partial_\nu\rho_\mu$, and g_s, g_c, g_w, g_r, A, and B are coupling constants. The nonlinear self-interaction of the σ meson is necessary to obtain an adequate behavior for the incompressibility around the saturation density.

Within a mean-field approximation, the equations of motion are

$$(i\ \partial\!\!\!/ - M + g_s\sigma + g_c\tau_3\phi - g_w\gamma_0\omega - g_r\gamma_0\tau_3\rho)\Psi = 0, \tag{5}$$

$$m_s^2\sigma + A\sigma^2 + B\sigma^3 = g_s\sum_j n_{sj}, \quad m_w^2\omega = g_w\sum_j n_j,$$
$$m_c^2\phi = g_c\sum_j I_j\,n_{sj}, \quad m_r^2\rho = g_r\sum_j I_j\,n_j.$$

As in the previous section, the density of particles with isospin projection j is represented by $n_j = \langle\bar{\Psi}_j\gamma_0\Psi_j\rangle$, whereas $n_{sj} = \langle\bar{\Psi}_j\Psi_j\rangle$ was used for the scalar density. They can be explicitly written as

$$n_j = \delta_s\int\frac{d^3p}{(2\pi)^3}f_j(p,\,T), \quad n_{sj} = \delta_s\int\frac{d^3p}{(2\pi)^3}f_j(p,\,T)\frac{m_j}{E_{pj}},$$

where $m_j = m - g_s\,\sigma - g_c I_j\phi$ is the in-medium effective mass and $E_{pj} = \sqrt{p^2 + m_j^2}$. Due to the assumed isotropy, only the zero component of the vector fields survives. Furthermore as there are no decaying channels between nucleons, only the third component of the isovectors contributes. The statistical distribution function $f_j(p,\,T)$ depends on the quasiparticle energies $\varepsilon_j = E_{pj} + g_w\omega + g_r I_j\rho$.

The energy density can be obtained by first evaluating the energy-momentum tensor and then taking mean values. In such a way, we obtain

$$\begin{aligned}\mathcal{E} = {}& \delta_s\sum_j\int\frac{d^3p}{(2\pi)^3}\,\varepsilon_j(p)f_j(p) + \frac{1}{2}m_s^2\sigma^2 \\ & + \frac{1}{2}m_c^2\phi^2 + \frac{1}{2}m_w^2\omega^2 + \frac{1}{2}m_r^2\rho^2 + \frac{A}{3}\sigma^3 + \frac{B}{4}\sigma^4.\end{aligned}$$

C. The low-density nuclear phase transition

The entropy density for a system in thermodynamical equilibrium is given by

$$\mathcal{S} = -\delta_s\sum_j\int\frac{d^3p}{(2\pi)^3}\,[f_j\ln f_j + (1-f_j)\ln(1-f_j)].$$

It can be used, together with the corresponding energy density $\mathcal{E}$, to evaluate the free energy density $\mathcal{F} = \mathcal{E} - T\mathcal{S}$ and the pressure $P = \sum_j\mu_j\,n_j - \mathcal{F}$ of the system.

A homogeneous system at temperature T and isospin composition n_1, n_2 remains thermodynamically stable if the free energy per unit volume $\mathcal{F}$ is lower than any linear combination of energies corresponding to independent thermodynamical states, say a and b, satisfying the conservation laws [10], i.e.,

$$\mathcal{F}(T,n_1,n_2) < \lambda\,\mathcal{F}\left(T,n_1^{(a)},n_2^{(a)}\right) + (1-\lambda)\,\mathcal{F}\left(T,n_1^{(b)},n_2^{(b)}\right). \tag{6}$$

Otherwise, the system becomes unstable and a change of phase is feasible. In such a case, two states can coexist if they verify the thermodynamical equilibrium conditions

$$P\left(T,n_1^{(a)},n_2^{(a)}\right) = P\left(T,n_1^{(b)},n_2^{(b)}\right), \tag{7}$$

$$\mu_1^{(a)} = \mu_1^{(b)}, \quad \mu_2^{(a)} = \mu_2^{(b)}. \tag{8}$$

Within the coexistence region, the total density of particles is a combination of contributions coming from each phase,

$$n_k = \lambda\,n_k^{(a)} + (1-\lambda)\,n_k^{(b)}, \quad 0<\lambda<1, \quad k=1,2, \tag{9}$$

where the λ parameter stands for the partial volume fraction of the phase a. As a consequence, if the system has global densities n_1, n_2, within the binodal region it could be composed of phases with densities differing considerably from the global values.

Any extensive thermodynamical quantity can be evaluated in a similar way: for instance the free energy can be written [10] $\mathcal{F}(T,n_1,n_2) = \lambda\,\mathcal{F}(T,n_1^{(a)},n_2^{(a)}) + (1-\lambda)\,\mathcal{F}(T,n_1^{(b)},n_2^{(b)})$.

In practice, we proceed as follows. For a given temperature T, we fix the pressure P_0 within a reasonable range. We explore this isobar and find a set of values $(n_1^{(a)},n_2^{(a)})$ and $(n_1^{(b)},n_2^{(b)})$ that fulfill Eq. (8). For these pairs of states we find all the solutions (n_1,n_2,λ) consistent with the requirement of Eq. (9). Exploring the range of temperatures and pressures for which there exist solutions of Eqs. (7)–(9), we obtain the binodal region immersed in a three-dimensional space, say $(T,\,P,\,w)$.

An interesting situation occurs for certain values of the variables $(T,\,P,\,w)$, for which the parameter λ does not exhaust the full range $[0,\,1]$. In such situations $\lambda = 0$ at low density, then it grows with the density, reaches a maximum value, and then comes back to zero. This phenomenon is known as the retrograde transition [10], because the system starts and ends

at the same phase but in between develops a germ of the other phase.

Within these prescriptions the thermodynamical potentials remain continuous throughout the phase transition. Discontinuities are relegated to their derivatives. Of special meaning are the heat capacity, compressibility, and thermal expansion coefficient. All of them are evaluated at constant particle number; for instance the heat capacity at constant volume is defined as $c_v = (\partial \mathcal{S}/\partial T)_{N_1,N_2,V}$.

Within the binodal this derivative must be evaluated carefully, since the total number of protons is distributed between the two coexisting phases. Furthermore, the parameter λ of Eq. (9) also has a temperature dependence that is not explicitly written. Taking these facts into account, and using $\mathcal{E}_a = \mathcal{E}(T, n_1^{(a)}, n_2^{(a)})$ and $\mathcal{E}_b = \mathcal{E}(T, n_1^{(b)}, n_2^{(b)})$, the heat capacity per unit volume in the binodal can be written

$$c_v(T,n_1,n_2) = \lambda \left(\frac{\partial \mathcal{E}_a}{\partial T}\right)_{n_1,n_2} + (1-\lambda)\left(\frac{\partial \mathcal{E}_b}{\partial T}\right)_{n_1,n_2} + (\mathcal{E}_a - \mathcal{E}_b)\left(\frac{\partial \lambda}{\partial T}\right)_{n_1,n_2}, \tag{10}$$

$$\left(\frac{\partial \mathcal{E}_c}{\partial T}\right)_{n_1,n_2} = R_c + \left(\frac{\partial \mathcal{E}_c}{\partial T}\right)_{n_1^{(c)},n_2^{(c)}}, \tag{11}$$

$$R_c = \sum_{k=1,2}\left(\frac{\partial \mathcal{E}_c}{\partial n_k^{(c)}}\right)_{T,n_j^{(c)}}\left(\frac{\partial n_k^{(c)}}{\partial T}\right)_{n_1,n_2}, \quad j \neq k. \tag{12}$$

The last term in Eq. (11) can be recognized as the heat capacity for a homogeneous system composed of only one phase $c_v^{(c)} = c_v(T, n_1^{(c)}, n_2^{(c)})$. Therefore, Eq. (10) can be summarized as

$$c_v(T,n_1,n_2) = \lambda c_v^{(a)} + (1-\lambda)c_v^{(b)} + \Delta c_v, \tag{13}$$

$$\Delta c_v = \lambda R_a + (1-\lambda)R_b + (\mathcal{E}_a - \mathcal{E}_b)\left(\frac{\partial \lambda}{\partial T}\right)_{n_1,n_2}. \tag{14}$$

When the system approaches the binodal boundary from inside, $\lambda \to 0$ or $\lambda \to 1$. For instance, $c_v(T,n_1,n_2) \to c_v^{(a)} + R_a + (\mathcal{E}_a - \mathcal{E}_b)(\partial\lambda/\partial T)_{n_1,n_2}$ when $\lambda \to 1$. Approaching the same point, but from outside the binodal, yields $c_v(T,n_1,n_2) \to c_v^{(a)}$. Hence we have a discontinuity $R_a + (\mathcal{E}_a - \mathcal{E}_b)(\partial\lambda/\partial T)_{n_1,n_2}$, where the first term contains several derivatives evaluated at the binodal boundary, while the second contribution is proportional to the energy difference between the coexisting phases. Expressions for the several derivatives appearing in Eqs. (10)–(12), can be found in the Appendix.

III. RESULTS AND DISCUSSION

In this section we show and discuss the results obtained for the binodal region and its thermodynamical properties as described by the selected models of the nuclear interaction. In particular we analyze the specific heat at constant volume throughout the phase transition, and in the case of symmetric nuclear matter we consider the definition of a latent heat and evaluate its temperature dependence.

For the Skyrme model the SLy4 parametrization is used, for which $t_0 = -2488.91$ MeV fm^3, $t_1 = 486.82$ MeV fm^5, $t_2 = -546.39$ MeV fm^5, $t_3 = 13777$ MeV fm$^{7/2}$, $x_0 = 0.834$, $x_1 = -0.344$, $x_2 = -1$, $x_3 = 1.354$, and $\gamma = 1/6$ [17].

For the QHD model with isovector mesons the parametrization given by Ref. [18] is used, for which $(g_s/m_s)^2 = 10.33$ fm^2, $(g_w/m_w)^2 = 5.42$ fm^2, $(g_c/m_c)^2 = 2.5$ fm^2, $(g_r/m_r)^2 = 3.15$ fm^2, $A/g_s^3 = 0.033$ fm^{-1}, and $B/g_s^4 = -0.0048$.

The saturation density, binding energy, incompressibility, and symmetry energy obtained are $n_0 = 0.159$ fm^{-3}, $E_B = -15.97$ MeV, $K = 229.9$ MeV, and $E_S = 32$ MeV in the Skyrme model, and $n_0 = 0.16$ fm^{-3}, $E_B = -16$ MeV, $K = 240$ MeV, and $E_S = 30.5$ MeV for the QHD model. Another significative quantity is the in-medium nucleon mass m^* at the saturation density: the values $m^*/m = 0.694$, and $m^*/m = 0.75$ are obtained for the Skyrme and QHD models, respectively.

First the binodal region is constructed for both models. Some results corresponding to the temperatures $T = 5$ and 10 MeV are shown in Fig. 1, in a plot of pressure versus proton abundance $y = (1-w)/2$. It can be seen that for the Skyrme

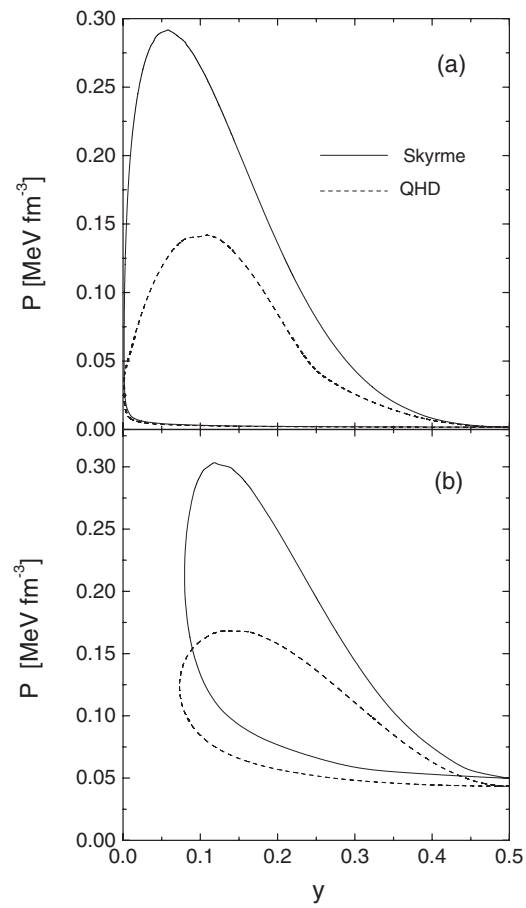

FIG. 1. Isothermal sections of the binodal corresponding to $T = 5$ MeV (a) and $T = 10$ MeV (b), for the selected models. The line convention specified in (a) is used for both cases.

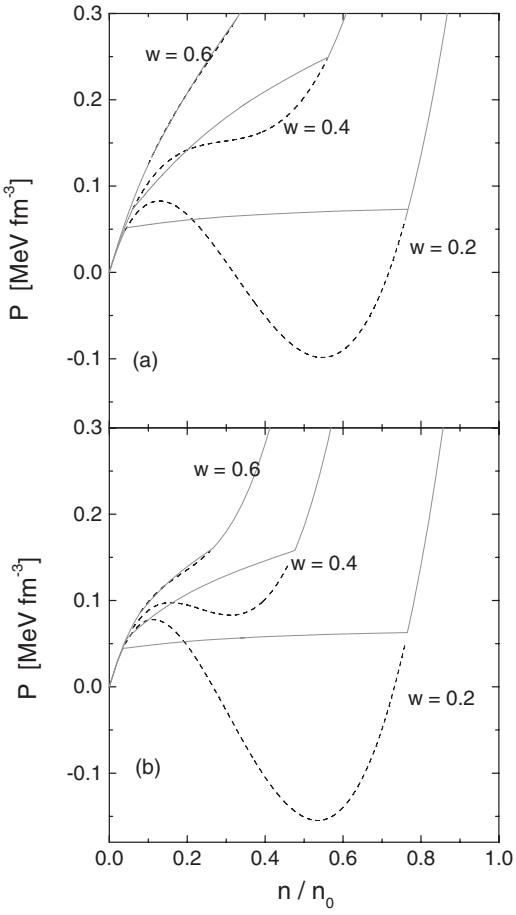

FIG. 2. The pressure as a function of the global density of particles corresponding to $T = 10$ MeV and several isospin asymmetries w, for the Skyrme (a) and QHD (b) models. Continuous lines correspond to physical states in thermodynamical equilibrium, dashed lines represent predictions of the models without the Gibbs construction.

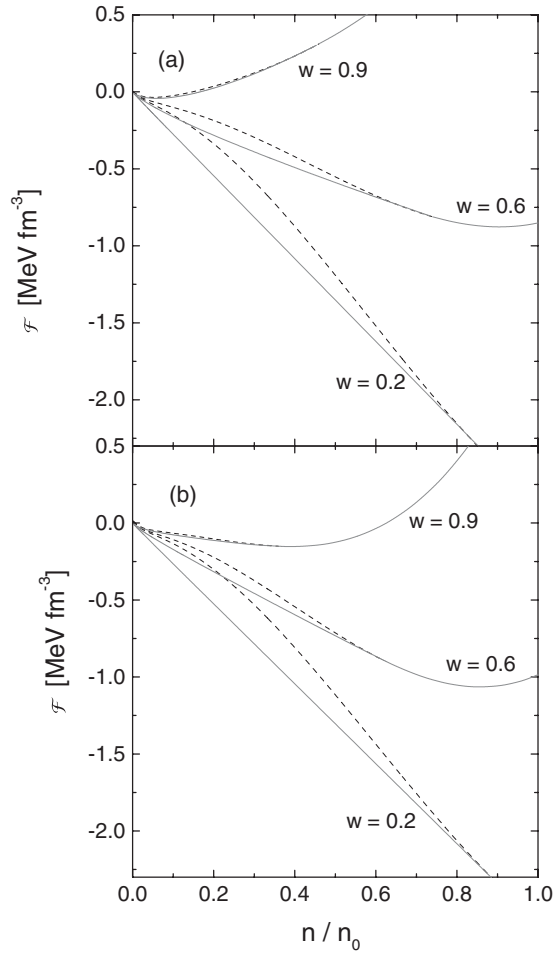

FIG. 3. The free energy density as a function of the global density of particles corresponding to $T = 5$ MeV and several isospin asymmetries w, for the Skyrme (a) and QHD (b) models. Continuous lines correspond to physical states in thermodynamical equilibrium, dashed lines represent predictions of the models without the Gibbs construction.

interaction that the coexistence of phases extends up to larger pressures. The range of temperatures is, instead, smaller. The critical temperatures are 14.5 and 15.9 MeV for Skyrme and QHD, respectively. It is worthwhile to mention that for high isospin asymmetries w (low y) the transition is of retrograde character. This situation can be appreciated more clearly in a plot of the pressure as a function of the global particle density, and several isospin asymmetries, as shown for $T = 10$ MeV in Fig. 2. Continuous lines correspond to the physical results, whereas dashed lines represent nonequilibrium states prior to the Gibbs construction. For high neutron excess ($w = 0.6$) the retrograde transition differs only slightly from the noncorrected pressure. In this circumstance, the mechanical stability condition ($\partial P/\partial n > 0$) is verified, but some of the matter diffusion conditions, $\partial\mu_1/\partial n > 0$ and $\partial\mu_2/\partial n < 0$, are not fulfilled. Furthermore, from the same figure it can be appreciated that, within the nonequilibrium region of highly asymmetric matter, the Skyrme model presents higher incompressibility than the QHD case. This is a consequence of the fast increase of the pressure while keeping almost unchanged densities, chemical potentials, and especially the derivatives of the chemical potentials. Hence, larger pressures are obtained in the former case within the range of densities that does not satisfy the equilibrium conditions. This fact explains why the binodal region extends up to larger pressures in the Skyrme model than in the QHD calculations, as shown in Fig. 1.

The effects of the Gibbs construction on the free energy are shown in Fig. 3. In order to ease the comparison, the rest-mass contribution has been removed from the QHD results. It can be corroborated that the coexistence of phases effectively minimizes the free energy, and changes its convexity also. For the temperature shown, $T = 5$ MeV, there is a retrograde transition for $w = 0.9$.

As a special case we consider matter to be globally isosymmetric; in such a case it behaves as a one-component system [10]. Along the phase separation the coexisting states have $w = 0$, and the pressure remains almost constant. In this sense the LGPT resembles a first-order transition. This circumstance can be appreciated in Fig. 4, where the density dependence of the pressure in the Skyrme model is shown for

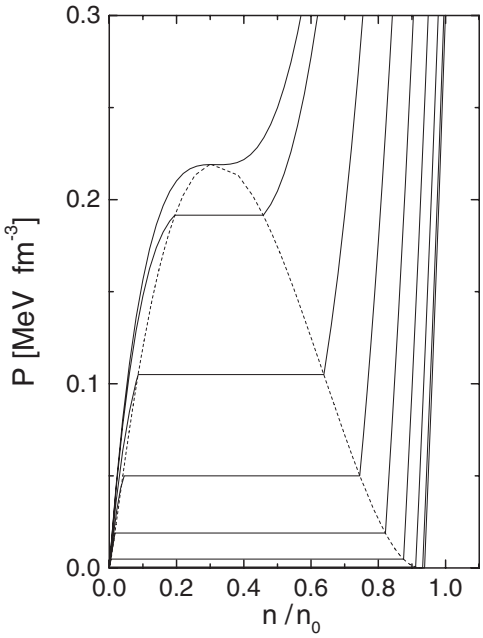

FIG. 4. The pressure for isospin symmetric nuclear matter as a function of the global density of particles, for a set of temperatures ranging from $T = 0$ to the critical temperature $T_c = 14.5$ MeV within the Skyrme model. The dashed line represent the boundary of the binodal.

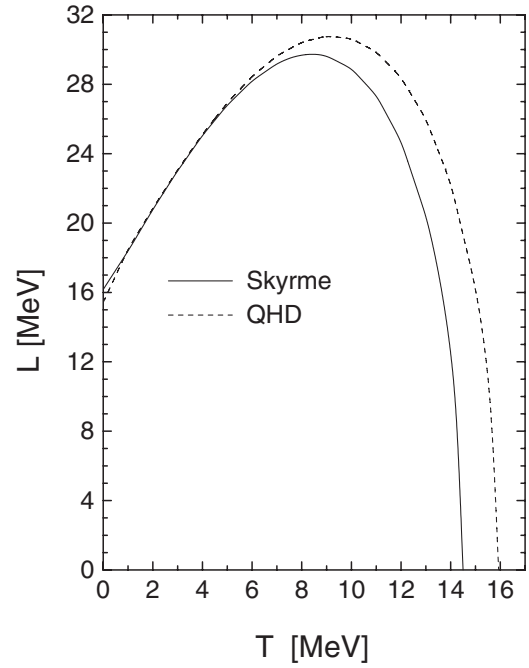

FIG. 5. The thermal dependence of L [see Eq. (15)], corresponding to the LGPT for symmetric nuclear matter, as given by the selected models.

several temperatures. The dashed line encloses the coexistence area. As was pointed out, there is no discontinuity in the thermodynamical potentials, and this is particularly true for the entropy. The difference $T\,[\mathcal{S}(T, n^{(a)}) - \mathcal{S}(T, n^{(b)})]$ represents the heat transferred as the LGPT is accomplished isothermically. It is interesting to compare this quantity with the latent heat corresponding to a first-order phase transition. It must be noted that some calculations find a first-order LGPT in the nuclear medium, even for two-components system. See for instance Ref. [13], where particle correlations beyond the mean-field approximation are included. Therefore the thermal dependence of this variation could be used to characterize the order of the change of phases.

In a recent paper [3] the latent heat for the LGPT in symmetric nuclear matter was studied for several parametrizations of the Skyrme model. In order to compare results, we consider the quantity

$$L = T\,(\mathcal{S}(T, n^{(a)})/n^{(a)} - \mathcal{S}(T, n^{(b)})/n^{(b)}) \qquad (15)$$

along an isothermal within the binodal, which coincides with the definition of the specific latent heat for a first-order transition. For a given temperature, the coexisting states with nucleon densities $n^{(a)}$ and $n^{(b)}$ are determined by the conditions of equal chemical potentials and pressures, so that L depends only on the temperature. In Fig. 5 the results obtained for the SLy4 parametrization and nonlinear QHD model are shown. The behavior is similar in both cases, with maximum values $L_{\max} = 29.7$ and 30.8 MeV for Skyrme and QHD forces, respectively. The value $L = 0$ is reached at the critical temperature. We corroborate some of the conclusions presented in Ref. [3]: (a) when $T \to 0$, L approaches to the binding energy at the saturation density; (b) for low temperatures L grows almost linearly; and (c) greater $L_{\max}$ corresponds to larger critical temperature.

Now we consider the specific-heat capacity at constant volume, evaluated according to Eqs. (10)–(12). First we examine the results for the Skyrme model, as shown in Fig. 6, where the density dependence of the heat capacity is displayed for several isospin asymmetries. Dashed lines represent the results obtained without the Gibbs construction. There are discontinuities at the thresholds of the binodal, as discussed at the end of Sec. II C. For a given temperature, the discontinuity decreases with the asymmetry w, as expected from the fact that pure neutron matter does not exhibit instabilities of the LGPT type. Within the binodal, c_v is a decreasing function of the density, in contrast to its behavior outside. Comparing the upper and lower panels of this figure, a general increment of around 60% is observed in the specific heat at $T = 10$ MeV compared to the $T = 5$ MeV outcome. For all the curves shown, there are jumps toward greater values of c_v as the system reaches the pure liquid state. The only exception occurs for the greater value of w shown in each figure, for which a retrograde transition takes place. A comparison with the results obtained using the QHD model can be made by examining Fig. 7. There is a general agreement with the previous description, with slightly greater values of c_v in the QHD case. In particular, for $T = 10$ MeV and $w = 0.6$, the curve for c_v does not show an appreciable discontinuity at the higher transition density $n = 0.47\,n_0$ because it is at the limit in the isospin asymmetry variable, separating full and retrograde evolution.

The thermal dependence of C_v is shown in Fig. 8 for some selected values of the global density and asymmetry. For this

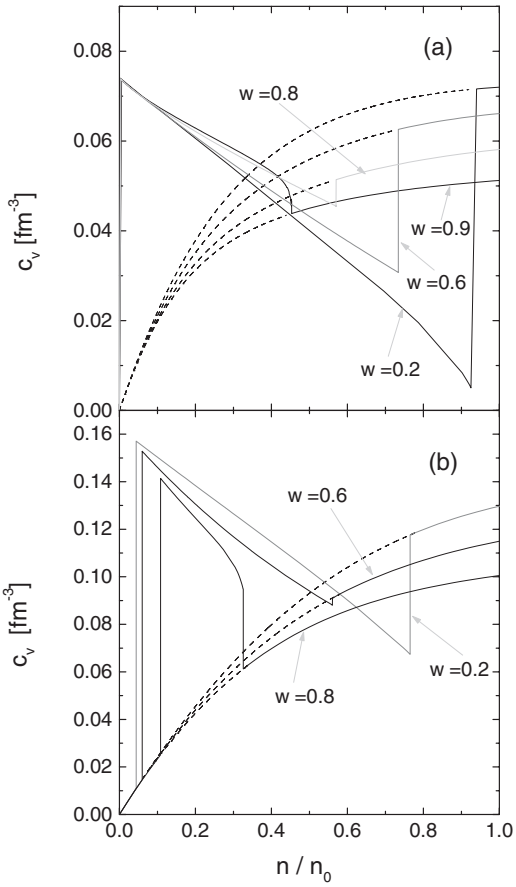

FIG. 6. The heat capacity per unit volume in terms of the global density of particles for several asymmetries w, corresponding to $T = 5$ MeV (a) and $T = 10$ MeV (b), within the Skyrme model. Continuous lines correspond to physical states in thermodynamical equilibrium, dashed lines represent predictions of the model without the Gibbs construction.

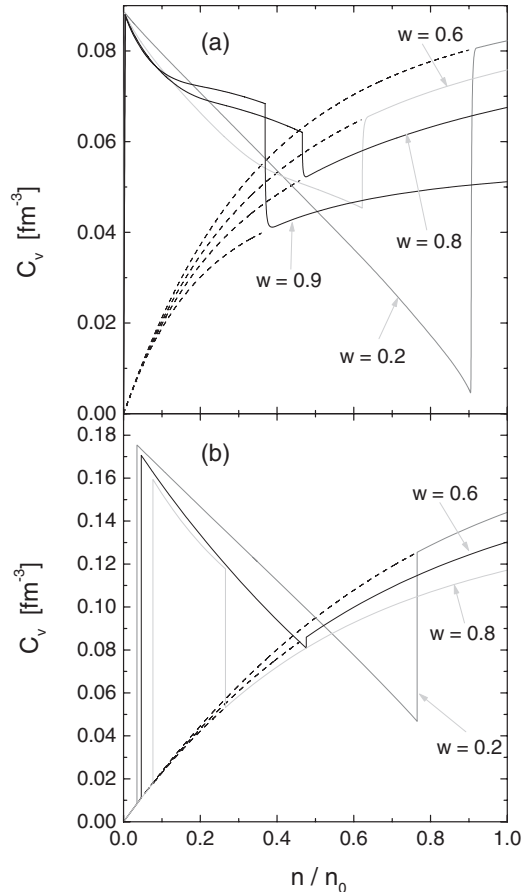

FIG. 7. The heat capacity per unit volume in terms of the global density of particles for several asymmetries w, corresponding to $T = 5$ MeV (a) and $T = 10$ MeV (b), within the QHD model. Continuous lines correspond to physical states in thermodynamical equilibrium, dashed lines represent predictions of the model without the Gibbs construction.

purpose we have chosen the Skyrme model, because the QHD results do not differ qualitatively. The heat capacity per particle exhibits an evident discontinuity of a few units at the threshold of the binodal. An increasing behavior is obtained for the full range of temperatures examined. As expected, this quantity approaches zero as the temperatures vanishes, according to the Nernst principle [19]. On the other hand, for high enough temperatures, the specific heat asymptotically approaches the noninteracting limit $3k_B/2$. The degree of convergence to this limit depends essentially on the global density n, with a negligible influence of the isospin asymmetry. The transition temperature is both a decreasing function of w (for fixed n) and n (for fixed w).

It can be observed that the magnitude of the discontinuity diminishes with both n and w. For the lowest density shown, $n/n_0 = 0.2$, the greatest jump corresponds to the lower isospin asymmetry $w = 0.2$ at $T \simeq 14$ MeV, and for the neutron-rich state $w = 0.8$ the discontinuity at $T \simeq 10.5$ MeV decreases by 60%.

The results shown in Fig. 8(a) can be contrasted with Fig. 6 of Ref. [13]. The comparison must be done cautiously since the latter used a canonical description for a high (but finite) number of particles in an inhomogeneous probe of nucleons. For $A = 1000$ the heat capacity increases slightly with temperature, up to a characteristic temperature $T \simeq 10$ MeV, where it reaches a peaked maximum. For higher T the heat capacity remains almost constant. The difference $\Delta C_v/N$ between the maximum and the plateau varies within the range 5–25, decreasing with the asymmetry w. In contrast, we obtain a high rate of growth before reaching the critical temperature, which is of the same order $T \simeq 10$ MeV. Furthermore, the drop from the peak to the plateau is less than 4. In our calculations the precise location of the temperature corresponding to the maximum decreases with w, in opposition to the behavior shown in Ref. [13].

IV. CONCLUSIONS

In this work we have examined the behavior of the heat capacity of infinite homogeneous nuclear matter in the region of low particle density and low temperature, taking the isospin composition as a relevant parameter. For this purpose we have selected two different descriptions of the nuclear interaction. Both the nonrelativistic Skyrme potential

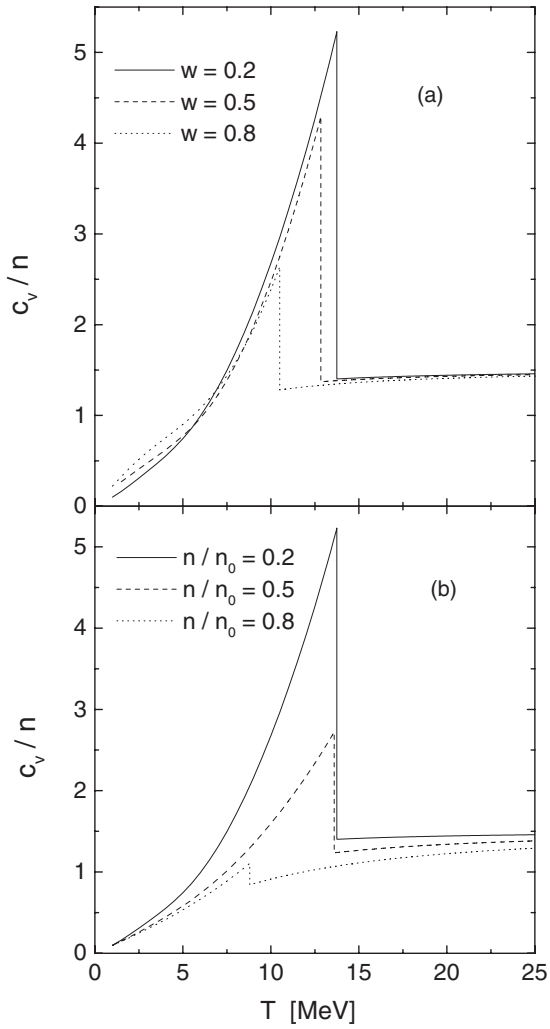

FIG. 8. The heat capacity per particle, within the Skyrme model, in terms of the temperature for $n/n_0 = 0.2$ and several isospin asymmetries w (a), and for fixed asymmetry $w = 0.2$ and several global densities (b).

and the field theoretical QHD model have been extensively used in the literature with remarkable success. Although these effective models have very different foundations, they describe appropriately the nuclear matter phenomenology for subsaturation densities.

We have examined the region of thermodynamical instability, where nuclear matter separates spontaneously into different phases. As we consider conservation of both neutron n_2 and proton n_1 densities, we found a three-dimensional region of the coexistence of phases. As a consequence, the thermodynamical potentials are continuous, leading to a second-order phase transition. Under these conditions, the heat capacity at constant volume has been particularly analyzed. As a first approximation we neglected the electromagnetic interaction, which could have significant influence on the thermodynamical fluctuations, leading to a change of phase; see for example Ref. [8]. The description obtained corresponds to a region of the phase space wider than in previous calculations, where more complex states of matter were considered [12,13].

The Gibbs construction allows conservation of the global densities of each isospin component through the coexistence of two phases with local densities differing appreciably from the global values n_1 and n_2. The relative abundance of each of these two phases can be represented through a parameter $0 < \lambda < 1$. The energy of the system is expressed as a linear combination of the energy of each phase, with coefficients λ and $1 - \lambda$. The evaluation of the heat capacity requires some care, since its definition prescribes derivatives at constant global densities, which does not imply fixed local densities. The temperature dependence of λ must also be considered.

We have found qualitative agreement between the predictions of both models. Only small differences can be found, for instance in the extension of the binodal region, the critical temperature, and the maximum value of the specific-heat capacity.

As expected in a second-order phase transition, the heat capacity exhibits a discontinuity at the boundary of the binodal. A detailed characterization of this discontinuity has been presented in terms of the thermodynamical variables for the full range of the coexistence of phases. For a fixed temperature we found a discontinuity at very low density and another one at a relatively greater value, corresponding to the transitions to pure gas and pure liquid, respectively. As the isospin asymmetry is increased, the full transition is replaced by a retrograde one. The high-density discontinuity in c_v has opposite behavior for each of these situations. For instance, in the retrograde evolution, c_v decreases suddenly when the matter leaves the coexistence region towards the pure liquid phase.

The thermal variation of the specific heat, at fixed density or isospin asymmetry, also shows a sharp but finite jump at a characteristic value. The location of this critical temperature decreases with both n and w. The magnitude of the discontinuity in the heat capacity per particle is less than 4, diminishing for increasing density and asymmetry.

As a special situation, we examined the change of phase for symmetric nuclear matter, which develops at very low pressures. In such a case we examined the entropy variation between the final states of an isothermal process within the binodal, and we have compared it with the latent heat L, defined for a first-order phase transition. As a function of temperature, $L(T)$ has a maximum value and vanishes for the critical temperature. We have found small differences between Skyrme and QHD predictions, and a general agreement with recently published results [3].

ACKNOWLEDGMENTS

This work was partially supported by CONICET, Argentina.

APPENDIX

The derivatives appearing in Eqs. (10) and (11) are obtained as solutions of a set of algebraic linear equations. We start by taking derivatives of Eqs. (9), keeping constants n_1 and n_2, for

$k = 1, 2$. After rearranging terms we obtain

$$0 = \left(n_1^{(a)} - n_1^{(b)}\right)\left[\lambda\frac{\partial n_2^{(a)}}{\partial T} + (1-\lambda)\frac{\partial n_2^{(b)}}{\partial T}\right] + \left(n_2^{(a)} - n_2^{(b)}\right)\left[\lambda\frac{\partial n_1^{(a)}}{\partial T} + (1-\lambda)\frac{\partial n_1^{(b)}}{\partial T}\right], \quad \text{(A1)}$$

$$\frac{\partial\lambda}{\partial T} = \left[\lambda\frac{\partial n_1^{(a)}}{\partial T} + (1-\lambda)\frac{\partial n_1^{(b)}}{\partial T}\right] \Big/ \left(n_1^{(a)} - n_1^{(b)}\right). \quad \text{(A2)}$$

In the next step, derivatives of Eqs. (8) are taken, giving

$$\left(\frac{\partial\mu_j^{(a)}}{\partial T}\right)_{n_1^{(a)},n_2^{(a)}} + \sum_{k=1,2}\left(\frac{\partial\mu_j^{(a)}}{\partial n_k^{(a)}}\right)_{n_l^{(a)},T}\frac{\partial n_k^{(a)}}{\partial T} = \left(\frac{\partial\mu_j^{(b)}}{\partial T}\right)_{n_1^{(b)},n_2^{(b)}} + \sum_{k=1,2}\left(\frac{\partial\mu_j^{(b)}}{\partial n_k^{(b)}}\right)_{n_l^{(b)},T}\frac{\partial n_k^{(b)}}{\partial T}, \quad \text{(A3)}$$

where $j = 1, 2$ and $l \neq k$. When there is no explicit statement, partial derivatives with respect to T are evaluated while holding the global densities n_1 and n_2 fixed.

Writing $P(T, n_1, n_2) = \sum_b \mu_b n_b - \mathcal{F}(T, n_1, n_2)$ before taking the derivative of Eq. (7) leads to

$$\sum_{j=1,2}\left(n_j^{(a)} - n_j^{(b)}\right)\left[\left(\frac{\partial\mu_j^{(a)}}{\partial T}\right)_{n_1^{(a)},n_2^{(a)}} + \sum_{k=1,2}\left(\frac{\partial\mu_j^{(a)}}{\partial n_k^{(a)}}\right)_{n_l^{(a)},T}\frac{\partial n_k^{(a)}}{\partial T}\right] = \mathcal{S}_b - \mathcal{S}_a \quad \text{(A4)}$$

with $\mathcal{S}_c = \mathcal{S}(T, n_1^{(c)}, n_2^{(c)})$.

Equations (A1)–(A4) constitute a set of five equations in the unknowns $\partial n_j^{(c)}/\partial T$, $j = 1, 2$, $c = a, b$, and $\partial\lambda/\partial T$. Some of the coefficients are model dependent; for instance in the Skyrme model we have

$$\left(\frac{\partial\mu_j^{(a)}}{\partial n_k^{(a)}}\right)_{n_l^{(a)},T} = \frac{\partial\tilde{\mu}_j^{(a)}}{\partial n_k^{(a)}} + (a_0 - I_j I_k a_2)/8 - \frac{\beta}{(8\pi)^2}\sum_i (b_0 + I_i I_j b_2)^2 H_{i3}^{(a)} + \frac{\gamma t_3 n_a^\gamma}{48}\left[3(\gamma+3) + 2w_a(1+2x_3)(I_k - I_j) + (1+2x_3)(1-\gamma)w_a^2\right] + \frac{\beta}{8\pi^2}\sum_i (b_0 + I_i I_j b_2) H_{i2}^{(a)}\frac{\partial\tilde{\mu}_i^{(a)}}{\partial n_l^{(a)}}, \quad l \neq k,$$

$$\frac{\partial\tilde{\mu}_j^{(a)}}{\partial n_k^{(a)}} = \left[4(I_j I_k - 1) + \beta(b_2 I_j I_k - b_0)H_{j2}^{(c)}\right]/8\,\beta\, H_{j1}^{(c)},$$

$$\left(\frac{\partial\mu_j^{(a)}}{\partial T}\right)_{n_1^{(a)},n_2^{(a)}} = \beta\left[\mu_j^{(a)} + \frac{v_j^{(a)}}{8} + \frac{\gamma t_3}{48}n^{(a)\,(1+\gamma)}\left[3 - (1+2x_3)w_a^2\right] - \frac{H_{j2}^{(a)}}{2m_j^{(a)}H_{j1}^{(a)}}\right] + \left(\frac{\beta}{4\pi}\right)^2\sum_k (b_0 + I_j I_k b_2)\left(H_{k3}^{(a)} - \frac{H_{k2}^{(a)\,2}}{H_{k1}^{(a)}}\right)\Big/ m_k^{(a)},$$

where the effective mass m_k and potential v_k have been given in Sec. II A, and

$$H_{jk}^{(a)} = \frac{1}{\pi^2}\int_0^\infty dp\, p^{2k} f_j\left(T, n_1^{(a)}, n_2^{(a)}\right)\left[1 - f_j\left(T, n_1^{(a)}, n_2^{(a)}\right)\right].$$

Furthermore

$$\left(\frac{\partial\mathcal{E}_a}{\partial T}\right)_{n_1^{(a)},n_2^{(a)}} = \left(\frac{\beta}{2\pi}\right)^2\sum_j\left(H_{j3}^{(a)} - \frac{H_{j2}^{(a)\,2}}{H_{j1}^{(a)}}\right)\Big/ m_j^{(a)},$$

$$\left(\frac{\partial\mathcal{E}_a}{\partial n_k^{(a)}}\right)_{n_l^{(a)},T} = \frac{n^{(a)}}{8}(a_0 - I_k w^{(a)}) + \frac{1}{4}\sum_j (b_0 + b_2 I_j I_k)K_j^{(a)} + \frac{\gamma t_3}{48}n^{(a)\,(1+\gamma)}\left[3 - (1+2x_3)w_a^2\right] - \frac{\beta}{8\pi^2}\sum_j\left[(b_0 + I_j I_k b_2)\left(H_{j3}^{(a)} + \frac{H_{j2}^{(a)\,2}}{H_{j1}^{(a)}}\right)\right]\Big/ m_j^{(a)} - \frac{1}{2}\sum_j (1 + I_j I_k)\frac{H_{j2}^{(a)}}{m_j^{(a)}H_{j1}^{(a)}}.$$

Similar calculations have been carried out within the QHD model, but in this case further complications arise because the interaction is mediated by the meson fields.

[1] B. K. Sharma and S. Pal, Phys. Rev. C **81**, 064304 (2010).
[2] A. Rios, Nucl. Phys. A **845**, 58 (2010).
[3] A. Carbone, A. Polls, A. Rios, and I. Vidaña, Phys. Rev. C **83**, 024308 (2011).
[4] C. Wu and Z. Ren, Phys. Rev. C **83**, 044605 (2011).
[5] M. Hempel, G. Pagliara, and J. Schaffner-Bielich, Phys. Rev. D **80**, 125014 (2009).
[6] M. Huang *et al.*, Phys. Rev. C **81**, 044618 (2010).
[7] D. G. Yakovlev and C. J. Pethick, Annu. Rev. Astron. Astrophys. **42**, 169 (2004).
[8] S. J. Lee and A. Z. Mekjian, Phys. Rev. C **63**, 044605 (2001); **68**, 014608 (2003); Phys. Lett. B **580**, 137 (2004).
[9] O. Y. Gnedin, D. G. Yakovlev, and A. Y. Potekhin, Mon. Not. R. Astron. Soc. **324**, 725 (2001).
[10] H. Muller and B. D. Serot, Phys. Rev. C **52**, 2072 (1995).
[11] J. Randrup and S. E. Koonin, Nucl. Phys. A **356**, 223 (1981).
[12] S. Das Gupta and A. Z. Mekjian, Phys. Rev. C **57**, 1361 (1998); C. B. Das, S. Das Gupta, and A. Z. Mekjian, *ibid*. **68**, 031601 (2003); K. A. Bugaev, M. I. Gorenstein, I. N. Mishustin, and W. Greiner, *ibid.* **62**, 044320 (2000); G. Chaudhuri and S. Das Gupta, *ibid.* **76**, 014619 (2007).
[13] C. B. Das, S. Das Gupta, and A. Z. Mekjian, Phys. Rev. C **67**, 064607 (2003).
[14] M. Bender and P. H. Heenen, Rev. Mod. Phys. **75**, 121 (2003).
[15] G. Baym and C. Pethick, *Landau Fermi Liquid Theory: Concepts and Applications* (Wiley-VCH, Weinheim, 2004).
[16] B. D. Serot and J. D. Walecka, Adv. Nucl. Phys. **16**, 1 (1986).
[17] F. Douchin, P. Haensel, and J. Meyer, Nucl. Phys. A **665**, 419 (2000).
[18] B. Liu, V. Greco, V. Baran, M. Colonna, and M. Di Toro, Phys. Rev. C **65**, 045201 (2002).
[19] H. B. Callen, *Thermodynamics and an Introduction to Thermostatistics* (Wiley, New York, 1985).